How to cite: *Angew. Chem. Int. Ed.* **2025**, *64*, e202418738
doi.org/10.1002/anie.202418738

Organometallic Chemistry

π-Lewis Base Activation of Carbonyls and Hexafluorobenzene

*Aditesh Mondal[+], Kevin Breitwieser[+], Sergi Danés, Annette Grünwald, Frank W. Heinemann, Bernd Morgenstern, Frank Müller, Michael Haumann, Maximilian Schütze, Dustin Kass, Kallol Ray, and Dominik Munz**

Abstract: We report hitherto elusive side-on η^2-bonded palladium(0) carbonyl (anthraquinone, benzaldehyde) and arene (benzene, hexafluorobenzene) palladium(0) complexes and present the catalytic hydrodefluorination of hexafluorobenzene by cyclohexene. The comparison with respective cyclohexene, pyridine and tetrahydrofuran complexes reveals that the experimental ligand binding strengths follow the order THF < C_6H_6 < C_6F_6 < cyclohexene < pyridine < benzaldehyde < anthraquinone. To understand this surprising order, the complexes' electronic structures were elucidated by nuclear magnetic resonance (NMR), single crystal X-Ray diffraction (sc-XRD), ultraviolet/visible (UV/Vis) electronic absorption, infrared (IR) vibrational, Pd L_3-edge X-ray absorption (XAS), and X-ray photoelectron (XP) spectroscopic techniques, complemented by Density Functional Theory (DFT) calculations including energy decomposition (EDA-NOCV) and effective oxidation state (EOS) analyses. For benzene, pyridine and cyclohexene, bonding follows the donor/acceptor picture of the Dewar–Chatt–Duncanson model. In stark contrast, hexafluorobenzene, benzaldehyde and anthraquinone bind via essentially the π-channel only and thus as π-analogues of Z-acceptor ligands. This contribution elucidates the control of functional-group selectivity in palladium(0) catalysis and delineates a novel strategy to activate electron-deficient π-systems.

Introduction

Palladium-olefin complexes[1] are intermediates in various industrial processes including olefin polymerization,[2] the Mizoroki-Heck reaction,[3] and the Wacker process.[4] Palladium also catalyzes the CH and CF functionalization of unsupported arenes, as well as the oxidation of cyclohexanones and aldehydes by dioxygen and/or quinones.[5] Recently, palladium(0) complexes emerged as privileged catalysts for carbon–carbon coupling of 1,3-dienes, 1,3-enynes and heteroarenes with imines, carbonyls, and Michael-acceptors.[6] This approach has been proposed to rely on the π-Lewis basicity of the soft metal, which renders the unsaturated substrate *nucleophilic*, whereas the well-established π-Lewis-acid activation (e.g. with Pd^{II} catalysts) leads to *electrophilic* reactivity.[7] The electronic structure of transition metal π-complexes[8] is typically rationalized by the Dewar–Chatt–Duncanson model,[9] which understands the interaction between the metal and the unsaturated ligand by a combination of σ-donation into a vacant *d*-orbital and π-backdonation from an occupied *d*-orbital (Figure 1, a).

In case of d^{10} configured metal complexes, where all *d*-orbitals are occupied, the bonding situation remains vague (Figure 1, b).[10] Also the metal's oxidation state remains unclear, as π-backdonation may oxidize the metal center.[11]

[*] Dr. A. Mondal,[+] Dr. K. Breitwieser,[+] Dr. A. Grünwald, Dr. D. Munz
Coordination Chemistry
Saarland University
Campus C4.1, D-66123 Saarbrücken, Germany
E-mail: dominik.munz@uni-saarland.de

S. Danés
Departament de Química, Institut de Química Computacional I Catàlisi
Universitat de Girona
c/m. Aurelia Capmany 69, 17003 Girona, Spain

Dr. A. Grünwald, Dr. F. W. Heinemann
Inorganic and General Chemistry
Friedrich-Alexander-Universität Erlangen-Nürnberg
Egerlandstr. 1, D-91058 Erlangen, Germany

Dr. B. Morgenstern
Solid State Chemistry
Saarland University
Campus C4.1, D-66123 Saarbrücken, Germany

Dr. F. Müller
Experimental Physics and Center for Biophysics
Saarland University
Campus E2.9, D-66123 Saarbrücken, Germany

Dr. M. Haumann
Fachbereich Physik
Freie Universität Berlin
Arnimallee 14, 14195 Berlin, Germany

M. Schütze, Dr. D. Kass, Dr. K. Ray
Institut für Chemie
Humboldt-Universität zu Berlin
Brook-Taylor-Straße 2, 12489 Berlin, Germany

[+] Both authors contributed equally to this work

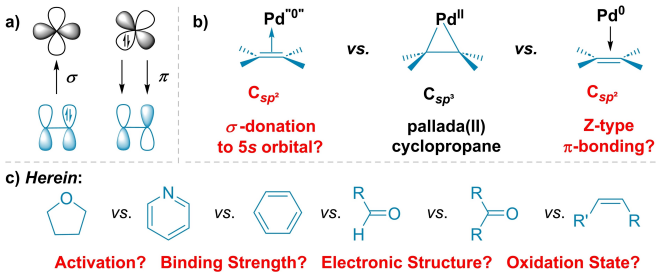

Figure 1. Bonding in metal–olefin complexes according to the Dewar–Chatt–Duncanson model (a), limiting resonance structures for low-valent palladium π-complexes (b), and ligands studied herein (c).

For nickel diphosphine-supported π-complexes, it has been argued instead that the metal merely channels electron density from the diphosphine to the π-ligand.[12] Note that intramolecular olefin-coordination to nickel may even give rise to ligand non-innocence.[13] In the third limiting case, and applying the covalent bond classification (CBC) method by Green and Parkin,[14] the metal–ligand bond could be understood as a Z-type interaction of a metal Lewis-base with a Lewis-acidic ligand. This perspective is commonly adopted for strong Lewis-acids in σ-symmetry.[15] Bonding of η^2-ligands by formally d^{10} configured metal complexes is particularly weak for delocalized π-systems and organic carbonyl compounds. Whereas a vast diversity of arene-complexes is known for transition metals with a *d*-electron count below 10,[16] essentially all corresponding (fluoro) arene[17] group 10 complexes relate to nickel. Note that the $4s^2d^8$ valence electron configuration of elemental nickel tentatively suggests higher Lewis acidity compared to elemental palladium and platinum with their $4d^{10}$ and $6s^15d^9$ valence shells.[18] Similarly, side-on η^2-coordination of the C=O[19] functionality is well established for nickel,[20] yet remains elusive for palladium, where only unproductive Werner-type κ^1-*O* end-on coordination is known. For instance, several side-on nickel(0) carbon dioxide complexes were crystallographically characterized.[21] In contrast, the only known palladium CO_2 complex is metastable in nature, and persists only at −30 °C even under an atmosphere of carbon dioxide.[22] In the (dibenzylideneacetone) palladium-(0) precursors $Pd_2(dba)_3$ and $Pd(dba)_2$, the dba ligands chelate the metal centers by their two olefinic groups, and no interaction with the carbonyl functionality is found.[23] Nitrosobenzene has been found to oxidize palladium(0), thereby affording a κ^1-*N* coordination.[24] With the exception of two examples with platinum(0) bisphosphine complexes, which form a side-on complex with $C_6(CF_3)_6$[25] and a $B(C_6F_5)_3$ adduct with CO_2,[26] reports on intermolecular[27] Pd and Pt η^2-arene and side-on R_2C=O complexes exclusively relate to binuclear palladium(I) scaffolds.[28] In fact, it has been hypothesized based on the elusiveness of such palladium complexes that the inferior functional group tolerance of the nickel cross-coupling catalysts might be rooted in the much higher binding strength with π-ligands.[29] Here, we report such palladium(0) π-complexes, their binding strengths, as well as their underlying electronic structure, which will allow to understand and rationally tailor functional group tolerance and selectivity in low-valent group 10 catalysis (Figure 1, c).

Results and Discussion

Synthesis

In a previous study,[30] we reported a palladium(0) pyridine complex supported by an imino-functionalized Cyclic (Alkyl)(Amino) Carbene (^{fun}CAAC) ligand ($\mathbf{1^{py}}$).[31] This complex serves as a powerful catalyst for transfer hydrogenation of ketones, amide formation from esters, borylation of alcohols and amines, and the dimerization of alkynes under exceedingly mild conditions.[30] This is because the pyridine is only weakly bound due to hard-soft mismatch, thus rendering the complex a $12e^-$ palladium(0) surrogate.[32] Consequently, $\mathbf{1^{py}}$ readily inserts into O–H, N–H, and C–C bonds even at room temperature,[33] and forms palladium terminal nitrenes with organic azides.[34] We presumed that the lability of the pyridine ligand in $\mathbf{1^{py}}$ should also provide the thermodynamic driving force for isolating η^2-carbonyl and arene complexes. Indeed, a substitution reaction to form **2** and **3**, as was evident from an immediate color change from deep red to orange-yellow, results upon treating benzene or pentane solutions of $\mathbf{1^{py}}$ with 2 equiv. of C_6F_6 or 1 equiv. of 4-isobutylbenzaldehyde (ald), respectively (Scheme 1). Similarly, adding 1 equiv. of anthraquinone (aq) led to a dark red solution associated with the formation of **4**. Complexes **2** and **4** precipitated quantitatively from the solution within 5 minutes, whereas **3** commenced to crystallize after 10 minutes. All three complexes were isolated analytically pure in high yields after washing with pentane and drying *in vacuo*. The ^{1}H NMR spectroscopic analysis revealed that although the C_6F_6 ligand in complex **2** stays attached to the metal center in tetrahydrofuran solutions, it undergoes quantitative ligand-exchange to $\mathbf{1^{C_6H_6}}$ upon dissolution in benzene (Figures S20–S23). Attempts to isolate $\mathbf{1^{C_6H_6}}$ through capture of pyridine by Lewis-acids were, however, unsuccessful and led to the formation of unknown mixtures.

Isolation attempts of the corresponding cyclohexene ($\mathbf{1^{C_6H_{10}}}$) and ethylene complexes ($\mathbf{1^{C_2H_4}}$),[34c] which formed cleanly in solution upon treating $\mathbf{1^{py}}$ with cyclohexene and ethylene, respectively, also afforded intractable mixtures of compounds. Single crystals suitable for X-Ray diffraction (sc-XRD) were obtained from the reaction mixture in case of **3** and **4**, whereas single crystals of **2** were obtained by diffusion of pentane into a saturated THF solution at room temperature.[35] The solid-state structures of the complexes **2**, **3**, and **4** revealed the side-on/η^2-coordination of the C=C (in **2** containing hexafluorobenzene) and C=O (in **3** and **4** containing 4-isobutylbenzaldehyde and anthraquinone, respectively) groups. Notably, the dangling imino group of the ^{fun}CAAC ligand in $\mathbf{1^{py}}$ coordinates the metal center in **2**, **3** and **4**. This is also the case in perdeutero-THF solutions according to the ^{13}C NMR spectroscopic analysis[31q] with signals for the imino-functionality appearing

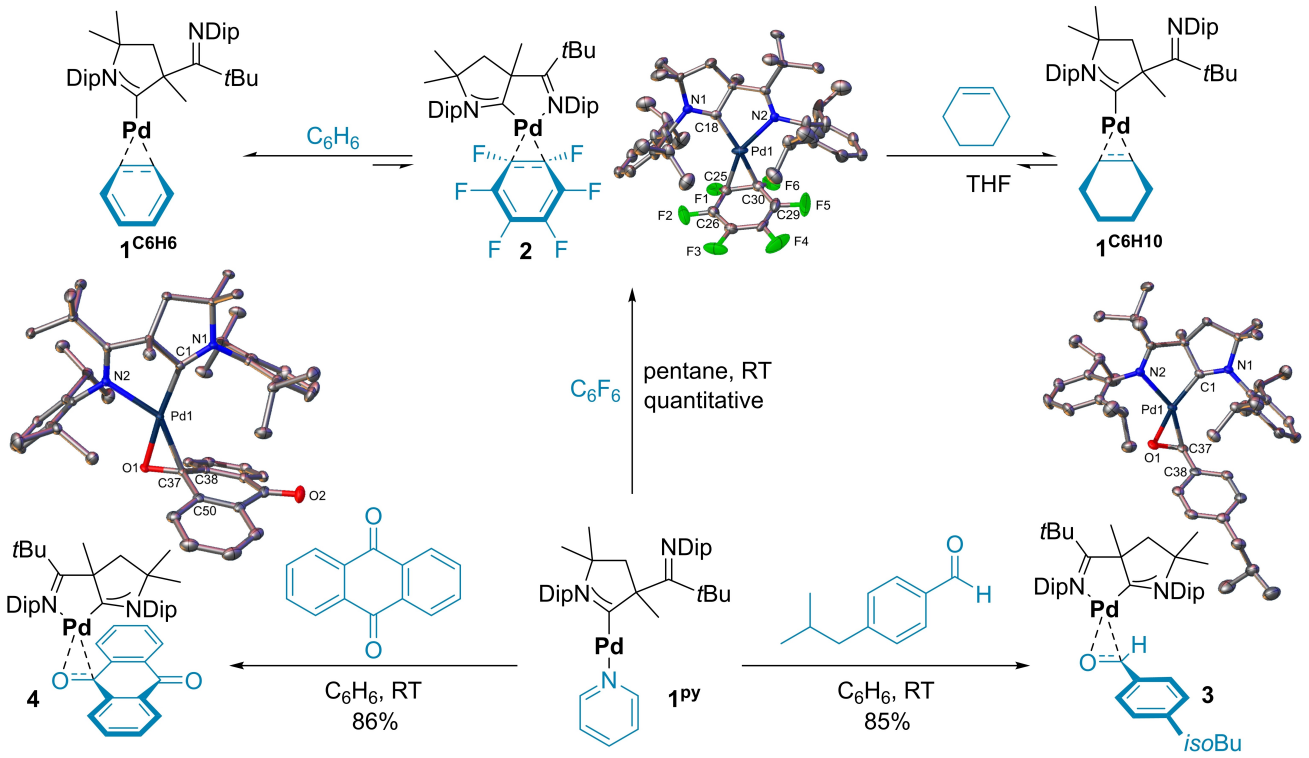

Scheme 1. Synthesis of palladium π-complexes **2**–**4** from the pyridine-coordinate precursor $\mathbf{1}^{py}$, their solid-state structures, and *in situ* generation of $\mathbf{1}^{C_6H_6}$ and $\mathbf{1}^{C_6H_{10}}$. Hydrogen atoms and co-crystallized solvent molecules are omitted for clarity, thermal ellipsoids are given at 50% probability. Selected bond lengths [Å] and angles [°]: **2**: Pd1–C18, 1.986(4); Pd1–C25, 2.098(11); Pd1–C30, 1.996(12); C25–F1, 1.379(13); C25–C26, 1.404(12); C25–C30, 1.464(8); C30–F6, 1.388(13); C30–C29, 1.435(12); Pd1–C25–F1, 117.5(6); Pd1–C25–C26, 119.4(10); Pd1–C30–F6, 117.2(7); Pd1–C30–C29, 118.3(9); F1–C25–C26, 113.8(9); F1–C25–C30, 114.2(10); F6–C30–C25, 116.6(9); F6 A–C30–C29, 110.7(10); C25–C30–C29, 116.7(12); C30–C25–C26, 118.1(12). **3**: Pd1–C1, 1.985(2); Pd1–O1, 2.0543(15); Pd1–C37, 2.065(2); O1–C37, 1.330(3); C37–C38, 1.480(3); Pd1–C37–C38, 118.00(16); Pd1–C37–O1, 70.73(12); O1–C37–C38, 119.4(2). **4**: Pd1–C1, 1.9881(12); Pd1–O1, 2.0231(9); Pd1–C37, 2.1795(12); O1–C37, 1.3274(15); C37–C38, 1.4758(17); C37–C50, 1.4822(18); Pd1–C37–O1, 65.28(6); Pd1–C37–C38, 115.40(8), Pd1–C37–C50, 114.64(8); O1–C37–C38, 118.79(11); O1–C37–C50, 118.87(11); C38–C37–C50, 114.60(11).

at 186.9 (**2**), 183.8 (**3**) and 185.9 ppm (**4**). Dissociation of the hemilabile imino group occurs for $\mathbf{1}^{C_6H_6}$ (172.7 ppm), just as is the case for $\mathbf{1}^{py}$ (173.0 ppm) and $\mathbf{1}^{C_6H_{10}}$ (172.3 ppm).[34a] Furthermore, a significant activation, that is elongation, of the pertinent C=C and C=O double bonds is evident in the solid state. In case of hexafluorobenzene, the bond length increases from 1.366 Å for free C_6F_6[36] to 1.464(8) Å in **2**. In **3**, the C=O bond elongates from 1.208(5) Å in cocrystallized benzaldehyde[37] to 1.330(3) Å, which is now closer to the 1.424(4)–1.436(4) Å found in *p*-methylbenzylalcohol crystals for the C–O single bond.[38] In the same manner, the coordinating C=O bond of anthraquinone in **4** elongates from 1.247(2) Å for the free ligand to 1.327(2) Å,[39] approaching the 1.448(2)–1.449(2) Å reported for a decorated 9,10-dihydroxyanthracenediol.[40] Similarly, one finds smaller bond angles centered on the coordinated carbon atoms, supporting a change in hybridization from sp^2 towards sp^3. For **2**, the F–C–C angles are 114.2(10)° and 116.6(9)°, which is closer to the 120° (117.1–122.6°) found for C_6F_6[36] than to the ideal tetrahedral angle of 109.5. For **4**, O–C–C angles of 118.79(11)° and 118.87(11)°, and a C–C–C angle of 114.60(11)° are observed, as compared to 120.2° and 119.6°, respectively, for free anthraquinone.[39] In case of **3**, the O–C–C angle is reduced from 125.8°[37] to 119.4(2)°. In line with reduced backbonding (see below), the Pd–C bonds to the ^{fun}CAAC ligands in **2** (1.986(4) Å), **3** (1.985 (2) Å) and **4** (1.9881(12) Å) are stretched compared to the Pd(0) complex $\mathbf{1}^{py}$ (1.926(3)–1.927(3) Å).[30] Note that corresponding four-coordinate Pd(II) complexes such as the dichloride (1.9230(19) Å) or the cyclic tosylimido complex (1.922(2) Å) show bond lengths comparable to $\mathbf{1}^{py}$.[34a] The IR-spectroscopic data for **3** ($\tilde{\nu}$ = 1598 cm^{-1}; free 4-isobutylbenzaldehyde; 1696 cm^{-1}) and **4** ($\tilde{\nu}$ = 1626, 1596 cm^{-1}; free anthraquinone: 1671 cm^{-1}) further corroborate substantial weakening of the C=O double bonds.

Ligand Exchange and Fluoride Metathesis

To quantify the relative strengths of the metal–ligand bonds in the complexes **1**–**4**, UV/Vis and ^{1}H NMR titration/exchange experiments were conducted (Scheme 2; Supporting Information).

Beyond THF,[41] the benzene ligand is most labile, followed by C_6F_6, which is stabilized by $\Delta G = 24 \pm 2$ kJ mol^{-1} in respect to benzene. Cyclohexene ($\Delta G = 1 \pm 0.1$ kJ mol^{-1}) and pyridine ($\Delta G = 4 \pm 1$ kJ mol^{-1}) follow. As the binding of hexafluorobenzene is weaker than that of pyridine, the

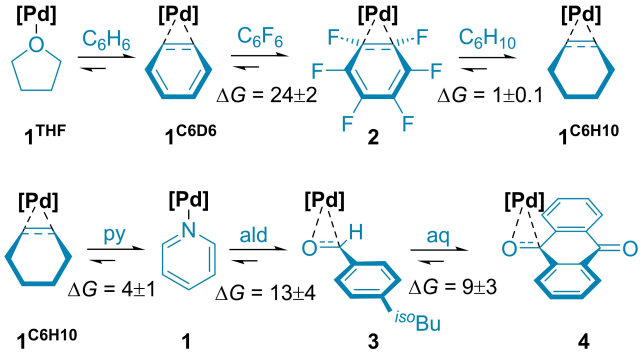

Scheme 2. Gibbs Free Energies ΔG (kJ mol^{-1}) for ligand exchange according to titrations in THF; ald, 4-isobutylbenzaldehyde; aq, anthraquinone.

synthesis of **2** from $\mathbf{1}^{py}$ is driven by precipitation of the product. Pyridine itself binds weaker ($\Delta G = -13 \pm 4$ kJ mol^{-1}) than 4-isobutylbenzaldehyde, whereas anthraquinone binds stronger ($\Delta G = 9 \pm 3$ kJ mol^{-1}). Interestingly, the trend neither follows the ligands' π-acidities nor anticipated metals' physical oxidation states (e.g., pyridine vs. C_6F_6). Ligand exchange was also modelled computationally at the ZORA-PBE0 (SMD)-D4/def2-TZVPP//ZORA-PBE0-D4/def2-SVP level of theory. The calculated Gibbs Free Energies ΔG (Figure S70) reproduce the experimental trend and equilibrium constants, thus validating the accuracy of the computational method.

Demonstrating the activation of hexafluorobenzene in a catalytic context, complex **2** was heated in the presence of further 9 equiv. of C_6F_6 and 10 equiv. of cyclohexene in tetrahydrofuran (Figure 2; Table S2). Beyond cyclohexane and benzene, pentafluorobenzene (~40 %, $TON = 4$; 50 equiv. substrate: $TON = 9$) as well as fluorocyclohexane (~15 %) and traces (~2 %) of 1,2,4,5- and 1,2,3,4-tetrafluorobenzene formed. Whereas the hydrodefluorination of electron-deficient fluoroarenes by hydridic reagents in the presence of late transition metal catalysts is well precedented,[42] this finding suggests that also metathesis-type approaches with allylic CH bonds are feasible.

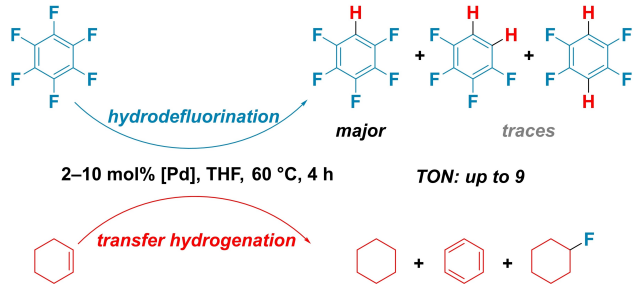

Figure 2. Catalytic hydrodefluorination of hexafluorobenzene by cyclohexene.

Computational Bonding Analysis: IBO, EOS, EDA-NOCV

We investigated the bonding situation of π-complexes **1**–**4** by state-of-the-art chemical bonding tools, namely Localized Orbital Bonding Analysis (LOBA) harnessing Intrinsic Bond Orbitals (IBOs), Energy Decomposition (EDA-NOCV), and Effective Oxidation State (EOS) analyses. Five IBOs representing occupied *d*-orbitals are found for **2**, **3** and **4**, which is consistent with a d^{10}-valence electron configuration (Figure 3, bottom). Four of these orbitals are exclusively localized at the palladium atoms (Table S7), whereas one *d*-orbital mixes with the ligand-centered π_L*-orbitals due to π-backbonding (Figure 3, top; $\mathbf{1}^{py}$, Pd:L = 0.89:0.11; $\mathbf{1}^{C_6H_6}$, Pd:L = 0.88:0.12; $\mathbf{1}^{C_6H_{10}}$, Pd:L = 0.86:0.14; **2**, Pd:L = 0.73:0.27; **3**, Pd:L 0.67:0.33; **4**, Pd:L = 0.60:0.40). The IBOs associated with the ligands' π_L donor orbitals representing the σ-donor interaction are ligand-centered and only moderately perturbed ($\mathbf{1}^{py}$, Pd:L = 0.10:0.90; $\mathbf{1}^{C_6H_6}$, Pd:L = 0.12:0.88; $\mathbf{1}^{C_6H_{10}}$, Pd:L = 0.10:0.90; **2**, Pd:L = 0.23:0.77; **3**, Pd:L = 0.10:0.90; **4**, Pd:L 0.12:0.88). The Effective Oxidation State Analysis (EOS; Table S16 and Figures S64–S69), using Topological Fuzzy Voronoi Cells (TFVC) further corroborates a Pd(0) oxidation state with confidences of 100 % ($\mathbf{1}^{py}$, $\mathbf{1}^{C_6H_6}$, $\mathbf{1}^{C_6H_{10}}$), 81 % (**2**), 75 % (**3**), and 66 % (**4**). Note that neither this order, nor the degree of IBO-covalency (*vide supra*) follow the experimentally determined order of ligand-exchange.

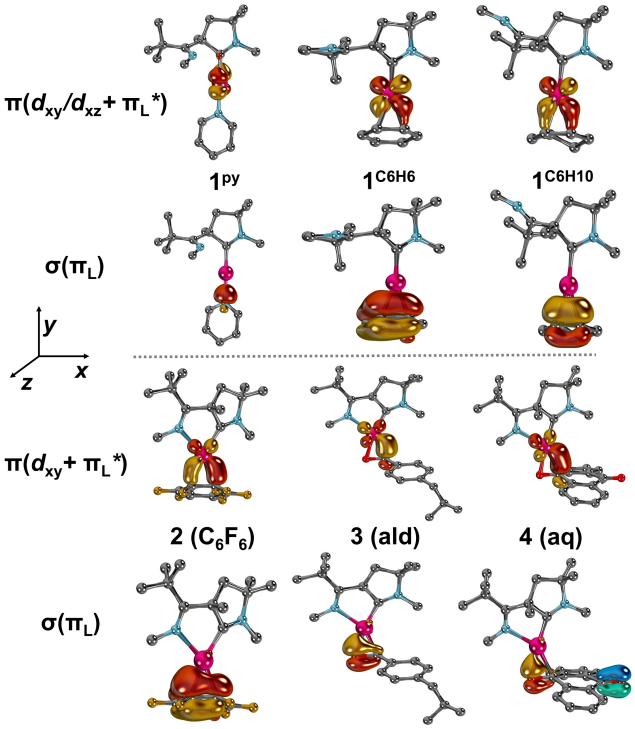

Figure 3. IBOs for the σ- and π-interactions of the metal with the ligand. For **4**, the π-orbital of the uncoordinated C=O bond (blue-green) is also shown for reference. For clarity, Dip groups (which have been included in the calculations) are truncated with methyl groups, and hydrogen atoms are omitted for clarity.

To understand the π-coordination from an energetic perspective, we analyzed the complexes through energy decomposition analysis (EDA-NOCV; Table 1). EDA further confirms oxidation states of zero for palladium (Tables S8, S9),[43] and the binding energies $-D_e$ are in line with the experiment.[44] The attractive interaction is composed of 45–65 % electrostatic and 30–47 % of orbital relaxation contribution. Dispersion (5–8 %) plays a minor role, yet becomes significant for anthraquinone ($\mathbf{1}^{\mathbf{C_6H_6}}$, $\Delta E_{disp} = -37.7$ kJ mol^{-1} vs. **4**, $\Delta E_{disp} = -76.7$ kJ mol^{-1}). The π-channel charge transfer $\Delta q_{Orb\text{-}\pi}$ (Hirshfeld atomic definitions) to the ligands (Tables S9–S15) follows the trend $\mathbf{1}^{\mathbf{py}}$ (0.05 a.u.) < $\mathbf{1}^{\mathbf{C_6H_6}}$ (0.18 a.u.) < $\mathbf{1}^{\mathbf{C_6H_{10}}}$ (0.24 a.u.) < **2** (0.54 a.u.) < **3** (0.62 a.u.) < **4** (0.75 a.u.). Most importantly, the EDA calculations partition the complexes into two groups, namely complexes **1** vs. complexes **2–4**. The preparation energies for $\mathbf{1}^{\mathbf{C_6H_6}}$ ($\Delta E_{prep} = +41.8$ kJ mol^{-1}), $\mathbf{1}^{\mathbf{C_6H_{10}}}$ ($\Delta E_{prep} = +48.5$ kJ mol^{-1}), and $\mathbf{1}^{\mathbf{py}}$ ($\Delta E_{prep} = +8.1$ kJ mol^{-1}) are small, in contrast to the large values calculated for the complexes **2–4** ($\Delta E_{prep} = 126.5$–172.8 kJ mol^{-1}), where the hemilabile imino group of ^{fun}CAAC coordinates the metal.

In line with modest charge transfer in the π-channel for complexes **1** (see above), the repulsive Pauli interaction is much stronger for complexes **2–4** ($\mathbf{1}^{\mathbf{C_6H_6}}$, $\Delta E_{Pauli} = +424.3$ kJ mol^{-1}; $\mathbf{1}^{\mathbf{C_6H_{10}}}$, $\Delta E_{Pauli} = +552.7$ kJ mol^{-1}; $\mathbf{1}^{\mathbf{py}}$, $\Delta E_{Pauli} = +325.5$ kJ mol^{-1} *vs.* **2**, $\Delta E_{Pauli} = +957.1$ kJ mol^{-1}; **3**, $\Delta E_{Pauli} = +710.7$ kJ mol^{-1}; **4**, $\Delta E_{Pauli} = +664.0$ kJ mol^{-1}). The splitting of the orbital interaction into NOCV bonding channels identifies the *d*–π* backbonding as the by far dominating orbital interaction for C_6F_6 (**2**), benzaldehyde (**3**), and anthraquinone (**4**; $\Delta E_{Orb\text{-}\pi} \approx 350$ kJ mol^{-1}, 69–77 %). The σ-donor interaction, which addresses mostly the vacant 5 *s* orbital (**2**, 71 %; **3**, 73 %; **4**, 69 % *s*-character; cf. Tables S9–S15) of the metal is almost as weak ($\Delta E_{Orb\text{-}\sigma} = 9$–$11$ %) as the commonly neglected[45] out-of-plane backbonding ($\Delta E_{Orb\text{-}\pi\perp} = 2$–$8$ %). In fact, the σ:π ratio exceeds 1:7, rendering the σ-donation essentially negligible. The exceedingly strong π-backbonding in complexes **2–4** furthermore leads to the coordination of the hemilabile imino-ligand, which compensates the electron-deficiency of the metal. Accordingly, we propose to understand the metal–ligand bond in complexes **2–4** as a Z-type interaction via the π-channel instead of the σ-channel as is usually the case.[46] Indeed, the energies associated with π-backbonding in **2–4** ($\Delta E_{Orb\text{-}\sigma} = -347.8$– -355.3 kJ mol^{-1}) exceed the σ-donation from a palladium center to a silicon-based Lewis-acid, which has been described as a *bona-fide* Z-ligand ($\Delta E_{Orb\text{-}\sigma} = -276$ kJ mol^{-1}),[47] by far.[48] In stark contrast, π-backbonding (33–47 %) and σ-bonding (21–36 %)

Table 1: EDA-NOCV of $\mathbf{1}^{\mathbf{C_6H_6}}$, $\mathbf{1}^{\mathbf{C_6H_{10}}}$, $\mathbf{1}^{\mathbf{py}}$, **2**, **3**, **4** at the ZORA-PBE0-D3(BJ)/TZ2P//ZORA-PBE0-D4/def2-SVP level of theory. Note that the hemilabile imino ligand is unbound in complexes **1**; see Table S8 and Figure S63 for a comparison with the tricoordinate complexes. Energies are given in [kJ mol^{-1}], charges in [a.u.].

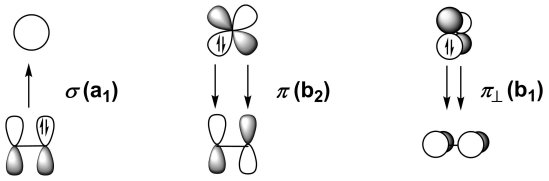

	$\mathbf{1}^{\mathbf{C_6H_6}}$	$\mathbf{1}^{\mathbf{C_6H_{10}}}$	$\mathbf{1}^{\mathbf{py}}$	**2** (C_6F_6)	**3** (ald)	**4** (aq)
$-D_e$	−93.0	−125.7	−123.5	−111.4	−157.0	−197.8
ΔE_{Prep}	+41.8	+48.5	+8.1	+172.8	+126.5	+136.7
ΔE_{int}	−134.8	−174.3	−131.6	−284.1	−286.3	−316.3
ΔE_{Pauli}	+424.3	+552.7	+325.5	+957.1	+710.7	+664.0
ΔE_{elstat}[a]	−327.6	−469.1	−322.3	−682.7	−479.4	−442.8
	(59 %)	(65 %)	(71 %)	(55 %)	(48 %)	(45 %)
ΔE_{Disp}[a]	−37.7	−38.3	−27.5	−57.1	−52.2	−76.7
	(7 %)	(5 %)	(6 %)	(5 %)	(5 %)	(8 %)
ΔE_{Orb}[a]	−194.5	−220.2	−107.5	−502.7	−466.4	−463.1
	(35 %)	(30 %)	(24 %)	(41 %)	(47 %)	(47 %)
$\Delta E_{HF\text{-}corr}$	+0.7	+0.7	+0.2	+1.4	+1.1	+2.4
$\Delta E_{Orb\text{-}corr}$[a]	−193.8	−219.5	−107.3	−501.3	−465.3	−460.8
	(35 %)	(30 %)	(23 %)	(40 %)	(47 %)	(47 %)
$\Delta E_{Orb\text{-}\pi}$[b]	−91.3	−126.4	−35.7	−347.8	−355.3	−353.2
	(47 %)	(58 %)	(33 %)	(69 %)	(76 %)	(77 %)
$\Delta E_{Orb\text{-}\sigma}$[b]	−40.8	−51.0	−39.2	−46.8	−50.8	−45.5
	(21 %)	(23 %)	(36 %)	(9 %)	(11 %)	(10 %)
$\Delta E_{Orb\text{-}\pi\perp}$[b,c]	−29.9	−11.8	−7.0	−41.2	−12.3	−11.7
	(15 %)	(5 %)	(7 %)	(8 %)	(3 %)	(2 %)
$\Delta E_{Orb\text{-}rest}$[b]	−31.8	−30.3	−25.4	−65.5	−46.9	−50.3
	(17 %)	(14 %)	(24 %)	(14 %)	(10 %)	(11 %)
$\Delta q_{Orb\text{-}\pi}$	0.18	0.24	0.05	0.54	0.62	0.75

[a] The values in parentheses give the percentage contribution to the total attractive interactions $\Delta E_{elstat} + \Delta E_{Disp} + \Delta E_{Orb} + \Delta E_{Orb\text{-}corr}$. [b] The values in paren the ses give the percentage contribution to the ΔE_{Orb}. [c] The orbital interaction of formally b_1 symmetry shows mixing with various other interactions, particularly for $\mathbf{1}^{\mathbf{C_6H_6}}$, $\mathbf{1}^{\mathbf{C_6H_{10}}}$, **2**.

are, albeit both weak, fairly balanced for complexes **1**. The donor/acceptor picture therefore describes the benzene, cyclohexene and pyridine ligands in **1** well in sight of a relative weight of about $<1:2$ of σ-bonding vs. π-back-bonding.

Experimental Bonding Analysis: UV/Vis, XPS, XAS, NMR

Ultraviolet/visible (UV/Vis) absorption measurements were performed in tandem with TD-DFT calculations to assign the electronic transitions in complexes **1**–**4** (Figures S71–S83). In line with the solid-state structures and computations, they classify the complexes into two groups. In compounds $\mathbf{1}^{py}$ ($\lambda_{exp}\approx580$ nm, $\lambda_{calc}=609$ nm), $\mathbf{1}^{C_6H_6}$ ($\lambda_{exp}\approx500$ nm; $\lambda_{calc}=500$ nm), and $\mathbf{1}^{C_6H_{10}}$ ($\lambda_{exp}\approx475$ nm; $\lambda_{calc}=480$ nm), the S1 excited states relate to a metal-to-ligand charge transfer (MLCT). These bands can be understood as HOMO→LUMO transitions from the metal's $d(z^2)$ orbital to the carbene's vacant π* orbital, and the transition energies follow the computed trend for the metals' physical oxidation states. For **2** (C_6F_6; $\lambda_{max}\approx450$ nm; $\lambda_{calc}=448$ nm) and **3** (ald; $\lambda_{max}\approx430$ nm; $\lambda_{calc}=424$ nm), the LUMO comprises not only the carbene, yet additionally the π-systems of the C_6F_6 and benzaldehyde ligands as well as (to a minor extent) of the coordinating imino-ligand. Consequently, the transition to the S1 excited state is also of mixed nature. In case of **4** (aq, $\lambda_{max}\approx512$ nm; $\lambda_{calc}=477$ nm), this transition addresses exclusively the anthraquinone ligand, that is the LUMO is here entirely centered at the η^2-ligand.

As the varying degree of 4*d* orbital mixing (cf. Figures S71–S83) renders the analysis of the underlying electronic structures ambiguous based on UV/Vis spectroscopy only, additional core-spectroscopies, namely palladium X-Ray photoelectron (XPS) and X-Ray absorption (XAS) spectral measurements were conducted. XPS was applied to gauge the metals' oxidation states (Figures S55–S60). These measurements were complicated by decomposition to palladium black within approximately 8 hours for complexes $\mathbf{1}^{py}$ and **2**, 6 h for complex **3**, and 2 h for complex **4**. Time dependent measurements suggest signals around 336.0 eV corresponding to the $3d_{5/2}$ level for all these complexes. This value is in the typical range for zero-valent palladium(0) complexes and close to the value for palladium foil (335.2 eV).[49] In case of complexes $\mathbf{1}^{py}$ and **2**, the analysis of the N1s (Figure S55) and F1s (Figure S57) signals right after sample preparation revealed that pyridine and hexafluorobenzene are partially removed under the experimental conditions with a low pressure of $<10^{-9}$ mbar. This observation confirms the labile nature of the pyridine and C_6F_6 ligands, and hence also a *bona-fide* oxidation state of zero. In short, although XPS measurements suggest that complexes $\mathbf{1}^{py}$, **2**, **3** and **4** feature oxidation states of 0, they did not allow for a comparative assessment of their physical oxidation states. L_3-edge XAS assesses the coordination environment of the metal and represents a sensitive method to gauge covalency in metal–ligand bonds.[50] Although it is comparatively underdeveloped for palladium, it, nevertheless, allowed to determine covalency in homoleptic chloropalladium complexes, as well as low-valent $PdAl_3$[51] and a heteroleptic palladium (I) amide.[52] Kennepohl and He also applied L-edge measurements to assess backbonding in η^2-coordinated nickel(0) complexes.[12a] The L_3-edge maximum energies (Figure 4) for **1**–**4** were observed at 3176.4 (**2**; C_6F_6), 3176.4 ($\mathbf{1}^{C_6H_{10}}$), 3176.2 ($\mathbf{1}^{C_6H_6}$), 3176.0 (**3**; benzaldehyde), 3176.0 ($\mathbf{1}^{py}$), and 3175.7 (**4**; anthraquinone) eV.

These energies do not follow an anticipated oxidation state trend, and shape and intensity of all edges are quite similar. Calculations at the DFT-ROCIS level (Figures S85–S90) were used to identify the nature of the transitions underlying the raising L_3-edge. In case of complexes **1**, they relate to transitions into the ^{fun}CAAC ligands' $p(z)$ orbitals, just as was the case for the UV/Vis spectra. In case of the aldehyde (**3**) and anthraquinone (**4**) complexes, they relate to transitions to the η^2-bonded ligands, with some contribution of the imine-ligand, whereas the transition in **2** mainly involves the imine ligand. Consequently, the L_3-edge data also classify the ligands into two groups (Figure 5). The

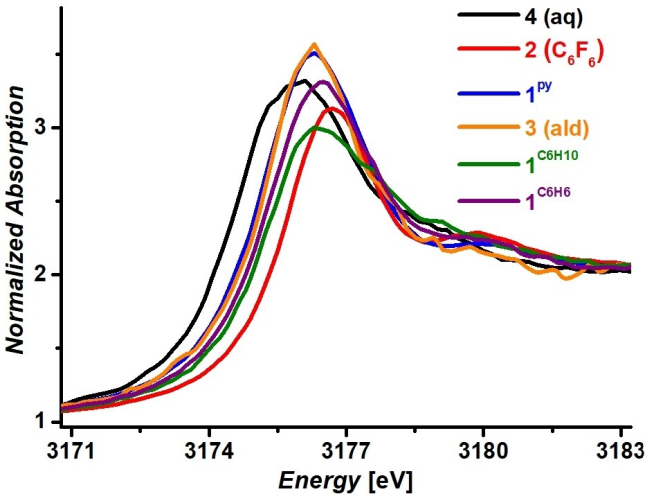

Figure 4. L_3-edge XAS spectra of $\mathbf{1}^{py}$, $\mathbf{1}^{C_6H_6}$, $\mathbf{1}^{C_6H_{10}}$, **2** (C_6F_6), **3** (ald) and **4** (aq).

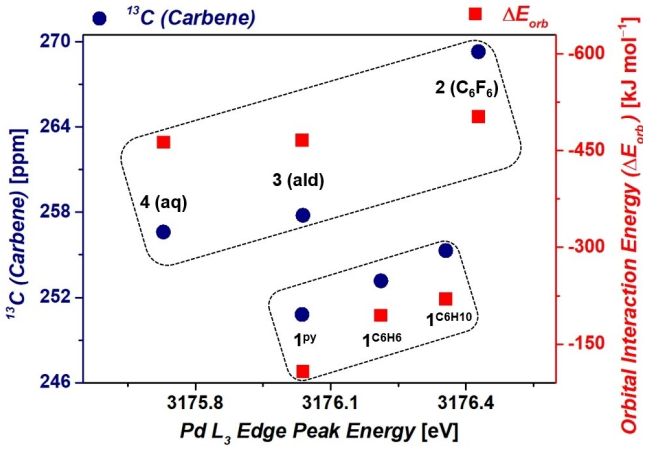

Figure 5. The ^{13}C carbene chemical shifts and overall orbital interaction energies ΔE_{Orb} correlate with the Pd L_3-edge peak energies.

trend of the decreasing edge energies reflects enhanced reduction of the metal with concomitantly enhanced π-backbonding to the ^{fun}CAAC in the order $\mathbf{1}^{py} > \mathbf{1}^{C_6H_6} > \mathbf{1}^{C_6H_{10}}$. In case of complexes **2**, **3** and **4**, the trend of the decreasing edge energies reflects the electrophilicity of the η²-bonded ligand, that is increasing metal(0) character and accordingly increasing backbonding to the ^{fun}CAAC in the order **4** < **3** < **2**. Donor properties of ligands in the *para*-position of carbenes may be assessed by the carbene's ^{13}C NMR shift (Huynh's electronic parameter).[53] Increasing overall donor-strength of the ligand in the *para*-positions thereby increasingly deshields the carbene atom's signal. Indeed, we find a correlation between the ^{13}C NMR shifts and the edge's peak energies (Figure 5, left).

This trend is also reproduced by the overall orbital interaction energy ΔE_{orb} for $\mathbf{1}^{py}$, $\mathbf{1}^{C_6H_6}$ and $\mathbf{1}^{C_6H_{10}}$ as obtained by the EDA-NOCV calculations (Figure 5, right), which is connected with the overall covalency of the metal–ligand bond. In case of the anthraquinone, aldehyde and hexafluorobenzene ligands, the covalency between the unsaturated ligand and the palladium metal is driven almost exclusively by π-backdonation. As such, the overall degree of covalency is well approximated by the covalency of the IBOs for complexes **2**, **3** and **4** relating to π-backdonation to the η²-bonded ligands only (Figure 6, left).

The same trend is found for calculated Hirshfeld charges at the metal, *viz.* the metal's physical oxidation state (Figure 6, right). For instance, anthraquinone is the strongest π-acceptor ligand (cf. Table 1); thus, the metal is most oxidized ($q = +0.32$ a.u.), the carbene carbon atom is the least deshielded ($\delta = 256.6$ ppm), and the L_3-edge peak energy is the lowest ($E = 3175.7$ eV) in sight of the energetically low-lying acceptor orbital at the anthraquinone ligand. In case of the pyridine, benzene, and cyclohexene complexes $\mathbf{1}^{py}$, $\mathbf{1}^{C_6H_6}$ and $\mathbf{1}^{C_6H_{10}}$, this trend is again reversed, because the acceptor orbital switches to the carbene, and because *both* σ- and π-effects are relevant. Pyridine for instance, which is both the weakest π-acceptor *and* σ-donor (cf. Table 1), leads to the physically lowest oxidation state ($q = 0.0$ a.u.), a moderately deshielded ^{13}C carbon atom ($\delta = 250.8$ ppm), as well as comparatively low L_3-edge peak energy ($E = 3176.0$ eV). In a nutshell, all spectroscopic data reveal that quinone, aldehyde and hexafluorobenzene act as Z-acceptor ligands, whereas pyridine, benzene and cyclohexene are to be understood as donor-acceptor ligands in the Dewar–Chatt–Duncanson sense.

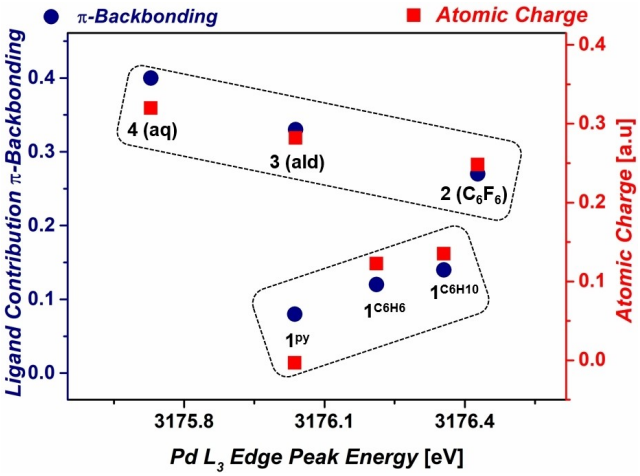

Figure 6. The covalency, i.e. degree of π-backbonding with the η²-bonded ligands according to IBOs, and Pd(0) character (Hirshfeld's atomic partial charges on the Pd atoms) correlate with the Pd L_3-edge peak energies.

Conclusions

This study reveals that bonding between palladium(0) and π-ligands may occur, opposed to common belief, by two different mechanisms. Specifically, bonding of palladium(0) with arenes, C=C, and C=O double bonds was elucidated. Side-on carbonyl (4-isobutyl benzaldehyde; anthraquinone) and arene (benzene, hexafluorobenzene) complexes were isolated and/or spectroscopically characterized (NMR, UV/Vis, IR, sc-XRD, XPS, XAS) for the first time, and put into context with an olefin (cyclohexene) as well as Werner-type (pyridine, THF) congeners. Ligand exchange experiments reveal metal–ligand bond strengths THF < C_6H_6 < C_6F_6 < cyclohexene < pyridine < 4-isobutylbenzaldehyde < anthraquinone. This order neither reflects the metals' physical oxidation states nor the ligands' Lewis-acidities, yet is rationalized by combined spectroscopic and computational data, which classify the ligands into two groups. Binding with THF, benzene, pyridine and cyclohexene occurs as a weak donor–acceptor interaction in the Dewar-Chatt Duncanson sense, where both σ- and π-effects are relevant, and where the weak σ-donation addresses the high-energy 5*s* orbital of the metal. In stark contrast, exceedingly strong backbonding at the expense of reorganization and Pauli-repulsion energy is found for benzaldehyde, quinone and hexafluorobenzene. This π-Lewis-base interaction effectively renders them Z-type ligands, thereby leading to strong activation of the multiple bond as was illustrated by the catalytic hydrodefluorination of hexafluorobenzene by cyclohexene. Thus, we present soft d^{10} metal complexes as straightforward-to-tune π-Lewis-bases for the selective activation of π-systems.

Supporting Information

The authors have cited additional references within the Supporting Information.[54–82]

Acknowledgements

We thank the funding from the European Research Council (ERC) under the European Union's Horizon 2020 Research and Innovation Program (grant no. 948185). Instrumentation and technical assistance for the sc-XRD analysis of **2** and **3** were provided by the Service Center X-ray Diffraction, with financial support from the Saarland University and the

German Science Foundation (DFG; Project INST 256/506-1 and 256/582-1), while sc-XRD analysis of **4** was performed at FAU Erlangen. We gratefully acknowledge scientific support and HPC resources provided by the Erlangen National High Performance Computing Center (NHR@FAU) of the Friedrich-Alexander-Universität Erlangen-Nürnberg (FAU). We thank the NHR funding provided by federal and Bavarian state authorities. The NHR@FAU hardware is partially funded by the German Research Foundation (DFG) – 440719683. We also thank the DFG for Germany's Excellence Strategy–EXC 2008–390540038–UniSysCat to K.R., D.K., and M.S. and the Heisenberg-Professorship to K.R. We thank the HZB for granting beamtime at KMC-3 at BESSY-II and I. Zizak and colleagues for technical support. Open Access funding enabled and organized by Projekt DEAL.

Conflict of Interest

The authors declare no conflict of interest.

Data Availability Statement

The data that support the findings of this study are available in the supplementary material of this article.

Keywords: Catalysis · Chemical Bonding · Intermediates · Organometallic Chemistry · Spectroscopy

[1] F. R. Hartley, *Chem. Rev.* **1969**, *69*, 799–844.
[2] L. K. Johnson, C. M. Killian, M. Brookhart, *J. Am. Chem. Soc.* **1995**, *117*, 6414–6415.
[3] a) I. P. Beletskaya, A. V. Cheprakov, *Chem. Rev.* **2000**, *100*, 3009–3066; b) A. Biffis, P. Centomo, A. Del Zotto, M. Zecca, *Chem. Rev.* **2018**, *118*, 2249–2295.
[4] R. I. McDonald, G. Liu, S. S. Stahl, *Chem. Rev.* **2011**, *111*, 2981–3019.
[5] a) X. Chen, K. M. Engle, D. H. Wang, J. Q. Yu, *Angew. Chem. Int. Ed.* **2009**, *48*, 5094–5115; b) S. S. Stahl, Y. Izawa, D. Pun, *Science* **2011**, *333*, 209–213; c) D. Wang, A. B. Weinstein, P. B. White, S. S. Stahl, *Chem. Rev.* **2017**, *118*, 2636–2679; d) A. E. Wendlandt, S. S. Stahl, *Angew. Chem. Int. Ed.* **2015**, *54*, 14638–14658.
[6] a) B. X. Xiao, B. Jiang, R. J. Yan, J. X. Zhu, K. Xie, X. Y. Gao, Q. Ouyang, W. Du, Y. C. Chen, *J. Am. Chem. Soc.* **2021**, *143*, 4809–4816; b) X. Yan, X.-M. Yang, P. Yan, B. Zhao, R. Zeng, B. Pan, Y.-C. Chen, L. Zhu, Q. Ouyang, *Chem. Sci.* **2023**, *14*, 4597–4604; c) B. Jiang, W.-T. Gui, H.-T. Wang, K. Xie, Z.-C. Chen, L. Zhu, Q. Ouyang, W. Du, Y.-C. Chen, *Chem. Sci.* **2023**, *14*, 10867–10874; d) G.-L. Shen, Y.-Y. Tan, Y. Hu, Z.-C. Chen, W. Du, Y.-C. Chen, *Org. Lett.* **2023**, *25*, 6649–6653; e) L. Zhu, B. Zhao, K. Xie, W.-T. Gui, S.-L. Niu, P.-F. Zheng, Y.-c. Chen, X.-W. Qi, Q. Ouyang, *Chem. Sci.* **2024**, *15*, 13032–13040.
[7] Z. C. Chen, Q. Ouyang, W. Du, Y. C. Chen, *J. Am. Chem. Soc.* **2024**, *146*, 6422–6437.
[8] a) T. Ziegler, A. Rauk *Inorg. Chem.* **1979**, *18*, 1558–1565; b) O. Eisenstein, R. Hoffmann, *J. Am. Chem. Soc.* **1981**, *103*, 4308–4320; c) K. Kitaura, S. Sakaki, K. Morokuma, *Inorg. Chem.* **1981**, *20*, 2292–2297; d) G. Frenking, N. Fröhlich, *Chem. Rev.* **2000**, *100*, 717–774; e) C. Goedecke, P. Hillebrecht, T. Uhlemann, R. Haunschild, G. Frenking, *Can. J. Chem.* **2009**, *87*, 1470–1479.
[9] a) J. Chatt, L. A. Duncanson, *J. Chem. Soc.* **1953**, 2939–2947; b) D. M. P. Mingos, *J. Organomet. Chem.* **2001**, *635*, 1–8; c) C. P. Gordon, R. A. Andersen, C. Copéret, *Helv. Chim. Acta* **2019**, *102*, e19001; d) T. Yang, Z. Li, X. B. Wang, G. L. Hou, *ChemPhysChem* **2023**, *24*, e202200835.
[10] a) C. Massera, G. Frenking, *Organometallics* **2003**, *22*, 2758–2765; b) Z. R. Wong, T. K. Schramm, M. Loipersberger, M. Head-Gordon, F. D. Toste, *Angew. Chem. Int. Ed.* **2022**, *61*, e202202019.
[11] M. Sircoglou, S. Bontemps, M. Mercy, N. Saffon, M. Takahashi, G. Bouhadir, L. Maron, D. Bourissou, *Angew. Chem. Int. Ed.* **2007**, *46*, 8583–8586.
[12] a) W. He, P. Kennepohl, *Faraday Discuss.* **2019**, *220*, 133–143; b) A. N. Desnoyer, W. He, S. Behyan, W. Chiu, J. A. Love, P. Kennepohl, *Chem. Eur. J.* **2019**, *25*, 5259–5268.
[13] a) M. L. G. Sansores-Paredes, M. Lutz, M.-E. Moret, *Nat. Chem.* **2024**, *16*, 417–425; b) M. L. G. Sansores-Paredes, T. T. T. Nguyen, M. Lutz, M.-E. Moret, *Organometallics* **2023**, *42*, 3418–3427; c) M. L. G. Sansores-Paredes, S. van der Voort, M. Lutz, M.-E. Moret, *Angew. Chem. Int. Ed.* **2021**, *60*, 26518–26522.
[14] a) M. L. H. Green, *J. Organomet. Chem.* **1995**, *500*, 127–148; b) M. L. H. Green, G. Parkin, *J. Chem. Educ.* **2014**, *91*, 807–816.
[15] a) J. Bauer, H. Braunschweig, R. D. Dewhurst, *Chem. Rev.* **2012**, *112*, 4329–4346; b) H. Braunschweig, R. D. Dewhurst, *Dalton Trans.* **2011**, *40*, 549–558; c) A. Amgoune, D. Bourissou, *Chem. Commun.* **2011**, *47*, 859–871; d) G. Bouhadir, D. Bourissou, *Chem. Soc. Rev.* **2016**, *45*, 1065–1079; e) D. You, F. P. Gabbaï, *Trends Chem.* **2019**, *1*, 485–496.
[16] a) E. O. Fischer, W. Hafner, *Z. Naturforsch. B: Chem. Sci.* **1955**, *10*, 665–668; b) E. O. Fischer, W. Hafner, *Z. Anorg. Allg. Chem.* **1956**, *286*, 146–148; c) I. U. Khand, G. R. Knox, P. L. Pauson, W. E. Watts, *J. Chem. Soc. Perkin Trans. 1* **1973**, 975–977; d) E. L. Muetterties, J. R. Bleeke, E. J. Wucherer, T. Albright, *Chem. Rev.* **1982**, *82*, 499–525; e) H. Schmidbaur, *Angew. Chem. Int. Ed.* **1985**, *24*, 893–904; f) D. Seyferth, *Organometallics* **2002**, *21*, 2800–2820; g) E. P. Kündig, *Transition Metal Arene π-Complexes in Organic Synthesis and Catalysis*, Springer-Verlag, Berlin Heidelberg, **2004**, pp. 1–232; h) M. Rosillo, G. Dominguez, J. Perez-Castells, *Chem. Soc. Rev.* **2007**, *36*, 1589–1604; i) G. Pampaloni, *Coord. Chem. Rev.* **2010**, *254*, 402–419; j) W. Huang, P. L. Diaconescu, *Chem. Commun.* **2012**, *48*, 2216–2218; k) J. Pahl, A. Friedrich, H. Elsen, S. Harder, *Organometallics* **2018**, *37*, 2901–2909; l) M. Schorpp, I. Krossing, *Chem. Sci.* **2020**, *11*, 2068–2076; m) P. Štarha, *Coord. Chem. Rev.* **2021**, *431*, 213690; n) S. M. Hubig, S. V. Lindeman, J. K. Kochi, *Coord. Chem. Rev.* **2000**, *200* (202), 831–873.
[17] a) R. G. Gastinger, K. J. Klabunde, *Transition Met. Chem.* **1979**, *4*, 1–13; b) S.-B. Choe, K. J. Klabunde, *J. Organomet. Chem.* **1989**, *359*, 409–418; c) K. J. Klabunde, B. B. Anderson, M. Bader, L. J. Radonovich, *J. Am. Chem. Soc.* **1978**, *100*, 1313–1314; d) I. Bach, K.-R. Pörschke, R. Goddard, C. Kopiske, C. Krüger, A. Rufińska, K. Seevogel, *Organometallics* **1996**, *15*, 4959–4966; e) J. Browning, C. S. Cundy, M. Green, F. G. A. Stone, *J. Chem. Soc. A* **1971**, 448–452; f) S. A. Johnson, E. T. Taylor, S. J. Cruise, *Organometallics* **2009**, *28*, 3842–3855; g) B. R. Barnett, C. E. Moore, P. Chandrasekaran, S. Sproules, A. L. Rheingold, S. DeBeer, J. S. Figueroa, *Chem. Sci.* **2015**, *6*, 7169–7178.
[18] R. Ugo, *Coord. Chem. Rev.* **1968**, *3*, 319–344.

[19] a) J. Kaiser, J. Sieler, D. Walther, E. Dinjus, L. Golic, *Acta Crystallogr. Sect. B: Struct. Sci.* **1982**, *38*, 1584–1586; b) T. T. Tsou, J. C. Huffman, J. K. Kochi, *Inorg. Chem.* **1979**, *18*, 2311–2317; c) I. Matas, J. Cámpora, P. Palma, E. Álvarez, *Organometallics* **2009**, *28*, 6515–6523; d) J. Cornella, E. Gomez-Bengoa, R. Martin, *J. Am. Chem. Soc.* **2013**, *135*, 1997–2009; e) T. J. Hadlington, T. Szilvasi, M. Driess, *Chem. Commun.* **2018**, *54*, 9352–9355; f) J. Duczynski, A. N. Sobolev, S. A. Moggach, R. Dorta, S. G. Stewart, *Organometallics* **2020**, *39*, 105–115; g) L. Tendera, T. Schaub, M. J. Krahfuss, M. W. Kuntze-Fechner, U. Radius, *Eur. J. Inorg. Chem.* **2020**, *2020*, 3194–3207.

[20] C. R. Work, V. M. Iluc, *in Comprehensive Coordination Chemistry III* (Eds.: E. C. Constable, G. Parkin, L. Que Jr), Elsevier, Oxford, **2021**, pp. 229–347.

[21] a) M. Aresta, C. F. Nobile, V. G. Albano, E. Forni, M. Manassero, *J. Chem. Soc. Chem. Commun.* **1975**, 636–637; b) A. Dohring, P. W. Jolly, C. Kruger, M. J. Romão, *Z. Naturforsch. B* **1985**, *40*, 484–488; c) J. S. Anderson, V. M. Iluc, G. L. Hillhouse, *Inorg. Chem.* **2010**, *49*, 10203–10207; d) B. M. Puerta Lombardi, C. Gendy, B. S. Gelfand, G. M. Bernard, R. E. Wasylishen, H. M. Tuononen, R. Roesler, *Angew. Chem. Int. Ed.* **2021**, *60*, 7077–7081; e) R. Beck, M. Shoshani, J. Krasinkiewicz, J. A. Hatnean, S. A. Johnson, *Dalton Trans.* **2013**, *42*, 1461–1475; f) Y.-E. Kim, J. Kim, Y. Lee, *Chem. Commun.* **2014**, *50*, 11458–11461.

[22] M. Sakamoto, I. Shimizu, A. Yamamoto, *Organometallics* **1994**, *13*, 407–409.

[23] a) C. G. Pierpont, M. C. Mazza, *Inorg. Chem.* **1974**, *13*, 1891–1895; b) M. C. Mazza, C. G. Pierpont, *Inorg. Chem.* **1973**, *12*, 2955–2959; c) M. C. Mazza, C. G. Pierpont, *J. Chem. Soc. Chem. Commun.* **1973**, 207b–208; d) A. R. Kapdi, A. C. Whitwood, D. C. Williamson, J. M. Lynam, M. J. Burns, T. J. Williams, A. J. Reay, J. Holmes, I. J. S. Fairlamb, *J. Am. Chem. Soc.* **2013**, *135*, 8388–8399; e) N. S. Kulikovskaya, E. E. Ondar, A. M. Perepukhov, A. Y. Kostyukovich, R. A. Novikov, V. P. Ananikov, *Inorg. Chem.* **2024**, *63*, 10527–10541.

[24] a) B. R. Barnett, J. S. Figueroa, *Chem. Commun.* **2016**, *52*, 13829–13839; b) L. A. Labios, M. D. Millard, A. L. Rheingold, J. S. Figueroa, *J. Am. Chem. Soc.* **2009**, *131*, 11318–11319.

[25] J. Browning, M. Green, J. L. Spencer, F. G. A. Stone, *J. Chem. Soc. Dalton Trans.* **1974**, 97–101.

[26] S. J. K. Forrest, J. Clifton, N. Fey, P. G. Pringle, H. A. Sparkes, D. F. Wass, *Angew. Chem. Int. Ed.* **2015**, *54*, 2223–2227.

[27] P. E. Rothstein, C. C. Comanescu, V. M. Iluc, *Chem. Eur. J.* **2017**, *23*, 16948–16952.

[28] For a monometallic Pd(I) CO complex, see: a) T. Bruckhoff, J. Ballmann, L. Gade, *Angew. Chem. Int. Ed.* **2024**, *63*, e202320064; for bimetallic Pd(I)–Pd(I) adducts, see: b) G. Allegra, G. Tettamanti Casagrande, A. Immirzi, L. Porri, G. Vitulli, *J. Am. Chem. Soc.* **1970**, *92*, 289–293; c) M. Gorlov, A. Fischer, L. Kloo, *J. Organomet. Chem.* **2004**, *689*, 489–492; d) T. Murahashi, M. Fujimoto, M. A. Oka, Y. Hashimoto, T. Uemura, Y. Tatsumi, Y. Nakao, A. Ikeda, S. Sakaki, H. Kurosawa, *Science* **2006**, *313*, 1104–1107; e) T. Murahashi, K. Takase, M. A. Oka, S. Ogoshi, *J. Am. Chem. Soc.* **2011**, *133*, 14908–14911.

[29] a) M. J. West, A. J. B. Watson, *Org. Biomol. Chem.* **2019**, *17*, 5055–5059; b) A. K. Cooper, P. M. Burton, D. J. Nelson, *Synthesis* **2019**, *52*, 565–573; c) A. K. Cooper, D. K. Leonard, S. Bajo, P. M. Burton, D. J. Nelson, *Chem. Sci.* **2020**, *11*, 1905–1911.

[30] A. Grünwald, F. W. Heinemann, D. Munz, *Angew. Chem. Int. Ed.* **2020**, *59*, 21088–21095.

[31] a) V. Lavallo, Y. Canac, C. Präsang, B. Donnadieu, G. Bertrand, *Angew. Chem. Int. Ed.* **2005**, *44*, 5705–5709; b) M. Soleilhavoup, G. Bertrand, *Acc. Chem. Res.* **2015**, *48*, 256–266; c) S. Roy, K. C. Mondal, H. W. Roesky, *Acc. Chem. Res.* **2016**, *49*, 357–369; d) M. Melaimi, R. Jazzar, M. Soleilhavoup, G. Bertrand, *Angew. Chem. Int. Ed.* **2017**, *56*, 10046–10068; e) U. S. D. Paul, U. Radius, *Eur. J. Inorg. Chem.* **2017**, *2017*, 3362–3375; f) R. Jazzar, M. Soleilhavoup, G. Bertrand, *Chem. Rev.* **2020**, *120*, 4141–4168; g) K. Breitwieser, D. Munz, *Adv. Organomet. Chem.* **2022**, *78*, 79–132; h) S. Kumar Kushvaha, A. Mishra, H. W. Roesky, K. Chandra Mondal, *Chem. Asian J.* **2022**, *17*, e202101301; i) D. Bourissou, O. Guerret, F. P. Gabbai, G. Bertrand, *Chem. Rev.* **2000**, *100*, 39–91; j) S. Diez-Gonzalez, N. Marion, S. P. Nolan, *Chem. Rev.* **2009**, *109*, 3612–3676; k) G. C. Fortman, S. P. Nolan, *Chem. Soc. Rev.* **2011**, *40*, 5151–5169; l) E. Peris, *Chem. Rev.* **2017**, *118*, 9988–10031; m) H. V. Huynh, *in The Organometallic Chemistry of N-heterocyclic Carbenes*, John Wiley & Sons, Ltd, **2017**, pp. 17–51; n) F. E. Hahn, *Chem. Rev.* **2018**, *118*, 9455–9456; o) D. Munz, *Organometallics* **2018**, *37*, 275–289; p) P. Bellotti, M. Koy, M. N. Hopkinson, F. Glorius, *Nat. Chem. Rev.* **2021**, *5*, 711–725; q) J. Chu, D. Munz, R. Jazzar, M. Melaimi, G. Bertrand, *J. Am. Chem. Soc.* **2016**, *138*, 7884–7887; r) D. Munz, J. Chu, M. Melaimi, G. Bertrand, *Angew. Chem. Int. Ed.* **2016**, *55*, 12886–12890; s) B. M. Puerta Lombardi, M. R. Faas, D. West, R. A. Suvinen, H. M. Tuononen, R. Roesler, *Nat. Commun.* **2024**, *15*, 3417; t) Y. Yamauchi, Y. Mondori, Y. Uetake, Y. Takeichi, T. Kawakita, H. Sakurai, S. Ogoshi, Y. Hoshimoto, *J. Am. Chem. Soc.* **2023**, *145*, 16938–16947.

[32] a) N. Marigo, B. Morgenstern, A. Biffis, D. Munz, *Organometallics* **2023**, *42*, 1567–1572; b) D. Munz, K. Meyer, *Nat. Chem. Rev.* **2021**, *5*, 422–439.

[33] K. Breitwieser, F. Dankert, A. Grünwald, P. R. Mayer, F. W. Heinemann, D. Munz, *Chem. Commun.* **2023**, *59*, 12104–12107.

[34] a) A. Grünwald, N. Orth, A. Scheurer, F. W. Heinemann, A. Pöthig, D. Munz, *Angew. Chem. Int. Ed.* **2018**, *57*, 16228–16232; b) S. J. Goodner, A. Grünwald, F. W. Heinemann, D. Munz, *Aust. J. Chem.* **2019**, *72*, 900–903; c) A. Grünwald, B. Goswami, K. Breitwieser, B. Morgenstern, M. Gimferrer, F. W. Heinemann, D. M. Momper, C. W. M. Kay, D. Munz, *J. Am. Chem. Soc.* **2022**, *144*, 8897–8901.

[35] Deposition Numbers 2372005 (for **2**), 2372004 (for **3**), 2351832 (for **4**) contain the supplementary crystallographic data for this paper. These data are provided free of charge by the joint Cambridge Crystallographic Data Centre and Fachin-formationszentrum Karlsruhe Access Structures service.

[36] N. Boden, P. P. Davis, C. H. Stam, G. A. Wesselink, *Mol. Phys.* **1973**, *25*, 81–86.

[37] L. Bao, P. Lv, T. Fei, Y. Liu, C. Sun, S. Pang, *J. Mol. Struct.* **2020**, *1215*.

[38] M. Hashimoto, M. Harada, M. Mizunoa, M. Hamada, T. Ida, M. Suhara, *Z. Naturforsch. A: Phys. Sci.* **2002**, *57*, 381–387.

[39] K. Lonsdale, J. Milledge, K. El Sayed, *Acta Crystallogr.* **1966**, *20*, 1–13.

[40] C. Krieger, A. R. Wartini, F. A. Neugebauer, *Acta. Crystallogr. Sect. C: Cryst. Struct. Commun.* **1998**, *54*, 1125–1127.

[41] No displacement of C_6F_6 was observed upon dissolving **2** in THF.

[42] a) M. F. Kuehnel, D. Lentz, T. Braun, *Angew. Chem. Int. Ed.* **2013**, *52*, 3328–3348; b) M. K. Whittlesey, E. Peris, *ACS Catal.* **2014**, *4*, 3152–3159; c) C. Hollingworth, V. Gouverneur, *Chem. Commun.* **2012**, *48*, 2929–2942.

[43] M. Gimferrer, S. Danés, E. Vos, C. B. Yildiz, I. Corral, A. Jana, P. Salvador, D. M. Andrada, *Chem. Sci.* **2023**, *14*, 384–392.

[44] The order of $\mathbf{1}^{\mathbf{py}}$ and $\mathbf{1}^{\mathbf{C_6H_{10}}}$, which show both computationally and experimentally very similar binding energies, is reversed, which we attribute to solvation effects.

[45] The orbital interaction of formally b_1 symmetry shows mixing with various other interactions, particularly in case of compound **2**. See the Supporting Information for further details.
[46] For other examples on π-only binding of transition metals with nitrenes or CO, see: a) W. Mao, D. Fehn, F. W. Heinemann, A. Scheurer, M. van Gastel, S. A. V. Jannuzzi, S. DeBeer, D. Munz, K. Meyer, *Angew. Chem. Int. Ed.* **2022**, *61*, e202206848; b) W. Mao, Z. Zhang, D. Fehn, S. A. V. Jannuzzi, F. W. Heinemann, A. Scheurer, M. van Gastel, S. DeBeer, D. Munz, K. Meyer, *J. Am. Chem. Soc.* **2023**, *145*, 13650–13662; c) M. Keilwerth, W. Mao, S. A. V. Jannuzzi, L. Grunwald, F. W. Heinemann, A. Scheurer, J. Sutter, S. DeBeer, D. Munz, K. Meyer, *J. Am. Chem. Soc.* **2023**, *145*, 873–887; d) M. Malischewski, K. Seppelt, J. Sutter, D. Munz, K. Meyer, *Angew. Chem. Int. Ed.* **2018**, *57*, 14597–14601.
[47] N. Ansmann, J. Munch, M. Schorpp, L. Greb, *Angew. Chem. Int. Ed.* **2023**, *62*, e202313636.
[48] H. Kameo, Y. Tanaka, Y. Shimoyama, D. Izumi, H. Matsuzaka, Y. Nakajima, P. Lavedan, A. Le Gac, D. Bourissou, *Angew. Chem. Int. Ed.* **2023**, *62*, e202301509.
[49] K. Breitwieser, M. Bevilacqua, S. Mullassery, F. Dankert, B. Morgenstern, S. Grandthyll, F. Müller, A. Biffis, C. Hering-Junghans, D. Munz, *Adv. Sci.* **2024**, 2400699.
[50] M. L. Baker, M. W. Mara, J. J. Yan, K. O. Hodgson, B. Hedman, E. I. Solomon, *Coord. Chem. Rev.* **2017**, *345*, 182–208.
[51] a) R. B. Boysen, R. K. Szilagyi, *Inorg. Chim. Acta* **2008**, *361*, 1047–1058; b) T. K. Sham, *Phys. Rev. B* **1985**, *31*, 1903–1908.
[52] J. Liu, M. M. Bollmeyer, Y. Kim, D. Xiao, S. N. MacMillan, Q. Chen, X. Leng, S. H. Kim, L. Zhao, K. M. Lancaster, L. Deng, *J. Am. Chem. Soc.* **2021**, *143*, 10751–10759.
[53] a) D. J. Nelson, S. P. Nolan, *Chem. Soc. Rev.* **2013**, *42*, 6723–6753; b) Q. Teng, H. V. Huynh, *Dalton Trans.* **2017**, *46*, 614–627; c) H. V. Huynh, *Chem. Rev.* **2018**, *118*, 9457–9492.
[54] F. A. Bovey, E. W. Anderson, F. P. Hood, R. L. Kornegay, *J. Chem. Phys.* **1964**, *40*, 3099–3109.
[55] A. A. Facundo, A. Arévalo, G. Fundora-Galano, M. Flores-Álamo, E. Orgaz, J. J. García, *New. J. Chem.* **2019**, *43*, 6897–6908.
[56] G. M. Sheldrick, *Acta Crystallogr. C Struct. Chem.* **2015**, *71*, 3–8.
[57] C. B. Hubschle, G. M. Sheldrick, B. Dittrich, *J. App. Crystallogr.* **2011**, *44*, 1281–1284.
[58] D. A. Shirley, *Phys. Rev. B* **1972**, *5*, 4709–4714.
[59] J. J. Yeh, I. Lindau, *At. Data Nucl. Data Tables* **1985**, *32*, 1–155.
[60] a) A. Onoda, Y. Tanaka, K. Matsumoto, M. Ito, T. Sakata, H. Yasuda, T. Hayashi, *RSC Adv.* **2018**, *8*, 2892–2899; b) T. Kondo, D. Guo, T. Shikano, T. Suzuki, M. Sakurai, S. Okada, J. Nakamura, *Sci. Rep.* **2015**, *5*, 16412.
[61] H. Dau, L. Iuzzolino, J. Dittmer, *Biochim. Biophys. Acta. Bioenerg.* **2001**, *1503*, 24–39.
[62] H. Dau, P. Liebisch, M. Haumann, *Anal. Bioanal. Chem.* **2003**, *376*, 562–583.
[63] a) F. Neese, *WIREs Comput. Mol. Sci.* **2022**, *12*, e1606; b) F. Neese, F. Wennmohs, U. Becker, C. Riplinger, *J. Chem. Phys.* **2020**, *152*, 224108; c) F. Neese, *Wiley Interdiscip. Rev.: Comput. Mol. Sci.* **2012**, *2*, 73–78.
[64] G. te Velde, F. M. Bickelhaupt, E. J. Baerends, C. Fonseca Guerra, S. J. A. van Gisbergen, J. G. Snijders, T. Ziegler, *J. Comput. Chem.* **2001**, *22*, 931–967.
[65] a) J. P. Perdew, M. Ernzerhof, K. Burke, *J. Chem. Phys.* **1996**, *105*, 9982–9985; b) C. Adamo, V. Barone, *J. Chem. Phys.* **1999**, *110*, 6158–6170; c) J. P. Perdew, K. Burke, M. Ernzerhof, *Phys. Rev. Lett.* **1996**, *77*, 3865–3868.
[66] J. D. Chai, M. Head-Gordon, *Phys. Chem. Chem. Phys.* **2008**, *10*, 6615–6620.
[67] a) S. Grimme, A. Hansen, S. Ehlert, J.-M. Mewes, *J. Chem. Phys.* **2021**, *154*, 064103; b) H. Kruse, S. Grimme, *J. Chem. Phys.* **2012**, *136*, 154101; c) E. Caldeweyher, S. Ehlert, A. Hansen, H. Neugebauer, S. Spicher, C. Bannwarth, S. Grimme, *J. Chem. Phys.* **2019**, *150*, 154122; d) J. W. Furness, A. D. Kaplan, J. Ning, J. P. Perdew, J. Sun, *J. Phys. Chem. Lett.* **2020**, *11*, 8208–8215.
[68] C. van Wüllen, *J. Chem. Phys.* **1998**, *109*, 392–399.
[69] F. Weigend, R. Ahlrichs, *Phys. Chem. Chem. Phys.* **2005**, *7*, 3297–3305.
[70] J. D. Rolfes, F. Neese, D. A. Pantazis, *J. Comput. Chem.* **2020**, *41*, 1842–1849.
[71] E. Caldeweyher, C. Bannwarth, S. Grimme, *J. Chem. Phys.* **2017**, *147*, 034112.
[72] a) F. Weigend, *Phys. Chem. Chem. Phys.* **2006**, *8*, 1057–1065; b) D. A. Pantazis, X.-Y. Chen, C. R. Landis, F. Neese, *J. Chem. Theory Comput.* **2008**, *4*, 908–919.
[73] V. Barone, M. Cossi, *J. Phys. Chem. A* **1998**, *102*, 1995–2001.
[74] A. V. Marenich, C. J. Cramer, D. G. Truhlar, *J. Phys. Chem. B* **2009**, *113*, 6378–6396.
[75] a) G. Knizia, J. E. Klein, *Angew. Chem. Int. Ed.* **2015**, *54*, 5518–5522; b) G. Knizia, *J. Chem. Theory Comput.* **2013**, *9*, 4834–4843.
[76] a) M. P. Mitoraj, A. Michalak, T. Ziegler, *J. Chem. Theory Comput.* **2009**, *5*, 962–975; b) A. Michalak, M. Mitoraj, T. Ziegler, *J. Phys. Chem. A* **2008**, *112*, 1933–1939.
[77] a) A. J. W. Thom, E. J. Sundstrom, M. Head-Gordon, *Phys. Chem. Chem. Phys.* **2009**, *11*, 11297–11304; b) I. F. Leach, J. E. M. N. Klein, *ACS Cent. Sci.* **2024**, *10*, 1406–1414.
[78] E. Van Lenthe, E. J. Baerends, *J. Comput. Chem.* **2003**, *24*, 1142–1156.
[79] E. P. A. Couzijn, Y.-Y. Lai, A. Limacher, P. Chen, *Organometallics* **2017**, *36*, 3205–3214.
[80] a) V. Postils, C. Delgado-Alonso, J. M. Luis, P. Salvador, *Angew. Chem. Int. Ed.* **2018**, *57*, 10525–10529; b) E. Ramos-Cordoba, V. Postils, P. Salvador, *J. Chem. Theory Comput.* **2015**, *11*, 1501–1508; c) M. Gimferrer, J. Van der Mynsbrugge, A. T. Bell, P. Salvador, M. Head-Gordon, *Inorg. Chem.* **2020**, *59*, 15410–15420.
[81] P. Salvador, E. Ramos-Cordoba, M. Montilla, L. Pujal, M. Gimferrer, *J. Chem. Phys.* **2024**, *160*, 17502.
[82] P. Salvador, E. Ramos-Cordoba, *J. Chem. Phys.* **2013**, *139*, 071103.

Manuscript received: September 28, 2024
Accepted manuscript online: December 23, 2024
Version of record online: January 10, 2025